Sea-ice and North Atlantic climate response to CO_2-induced warming and cooling conditions

Larissa NAZARENKO,[1] Nickolai TAUSNEV,[2] James HANSEN[3]

[1]*Columbia University/NASA Goddard Institute for Space Studies, 2880 Broadway, New York, New York 10025, USA*
E-mail: lnazarenko@giss.nasa.gov
[2]*SGT Incorporated/NASA Goddard Institute for Space Studies, 2880 Broadway, New York, New York 10025, USA*
[3]*NASA Goddard Institute for Space Studies, 2880 Broadway, New York 10025, New York, USA*

ABSTRACT. Using a global climate model coupled with an ocean and a sea-ice model, we compare the effects of doubling CO_2 and halving CO_2 on sea-ice cover and connections with the atmosphere and ocean. An overall warming in the $2 \times CO_2$ experiment causes reduction of sea-ice extent by 15%, with maximum decrease in summer and autumn, consistent with observed seasonal sea-ice changes. The intensification of the Northern Hemisphere circulation is reflected in the positive phase of the Arctic Oscillation (AO), associated with higher-than-normal surface pressure south of about 50° N and lower-than-normal surface pressure over the high northern latitudes. Strengthening the polar cell causes enhancement of westerlies around the Arctic perimeter during winter. Cooling, in the $0.5 \times CO_2$ experiment, leads to thicker and more extensive sea ice. In the Southern Hemisphere, the increase in ice-covered area (28%) dominates the ice-thickness increase (5%) due to open ocean to the north. In the Northern Hemisphere, sea-ice cover increases by only 8% due to the enclosed land/sea configuration, but sea ice becomes much thicker (108%). Substantial weakening of the polar cell due to increase in sea-level pressure over polar latitudes leads to a negative trend of the winter AO index. The model reproduces large year-to-year variability under both cooling and warming conditions.

1. INTRODUCTION

Global warming due to increased atmospheric CO_2 and other greenhouse gases has been held responsible for dramatic changes in the Arctic climate during the past two decades. The Arctic sensitivity to increased concentrations of greenhouse gases is amplified by positive sea-ice albedo feedback (Manabe and others, 1992; Randall and others, 1998; Holland and Bitz, 2003) and by an increase in high-latitude cloud cover (Curry and others, 1996). The observational evidence indicates that variability in sea ice tends to be connected with large-scale geographical patterns of atmospheric circulation, such as the North Atlantic Oscillation (NAO) and the Arctic Oscillation (AO), which have shown trends towards the high index phase over the past few decades (Fang and Wallace, 1994; Slonosky and others, 1997; Deser and others, 2000; Dickson and others, 2000; Walsh and others, 2002; Belchansky and others, 2005; Rigor and others, 2006). Sea-ice cover over the Arctic has declined by about 3% per decade since 1979 (Comiso, 2002; Parkinson and Cavalieri, 2002). Extensive sea-ice melting affects the stability of the ocean column, which can contribute to the strength of deep water formation and to the intensity of the meridional overturning circulation (MOC) in the North Atlantic. Changes in the poleward ocean heat transport at high latitudes, which are part of the MOC, can modify the sea-ice extent.

Under cooling conditions sea-level pressure (SLP) increases over high northern latitudes (Rind, 1998). This causes strengthening of the anticyclonic atmospheric circulation over the central Arctic, southwesterly flow across the subtropical Atlantic and weakening westerly flow across the North Atlantic. The precipitation pattern is consistent with a low AO index phase: reduced precipitation over the Arctic, northern Europe and Russia, and increased precipitation over southern Europe, the Mediterranean and northern Africa.

In this study, we focus on comparison of responses to increased and decreased CO_2. Responses considered are sea-ice changes and connections with hemispheric changes in the atmospheric circulation, surface air temperature (SAT) and the Atlantic MOC. Numerical experiments with doubled and halved CO_2 concentration are conducted for simulated periods of 120 years. Changes relative to a control are considered for the last 40 year averages. A timescale of 100 years was chosen in accordance with the Intergovernmental Panel on Climate Change (Houghton and others, 2001) emphasis for definitions for global warming potentials. On this timescale, the ocean heat transport, the ocean mixed layer, the sea-ice distribution and atmospheric circulation partially adjust to the applied warming or cooling conditions.

2. MODEL DESCRIPTION

We use the NASA Goddard Institute for Space Studies (GISS) Global Climate Model (GCM) Model III version (Schmidt and others, 2006) with 4 by 5° horizontal resolution and 20 vertical layers, with the model top at 0.1 hPa. The physics of this model is similar to the model used in the climate studies of Hansen and others (2002) but includes some improvements as reported by Schmidt and others (2006). We also use a dynamic ocean model with the same horizontal resolution as the GCM; it has 13 vertical levels, with finer resolution in the top 100 m. The ocean model includes the K-profile parameterization (KPP; Large and others, 1994) for vertical mixing and Gent and McWilliams' (1990) parameterization for mixing effect associated with mesoscale eddies. We use a sea-ice model, which includes both dynamics and thermodynamics of the ice cover in the Arctic and Antarctic. We employ no flux correction in the heat exchange between atmosphere and ocean. A control experiment for AD 1880 atmospheric composition exhibited

https://doi.org/10.3189/172756506781828566 Published online by Cambridge University Press

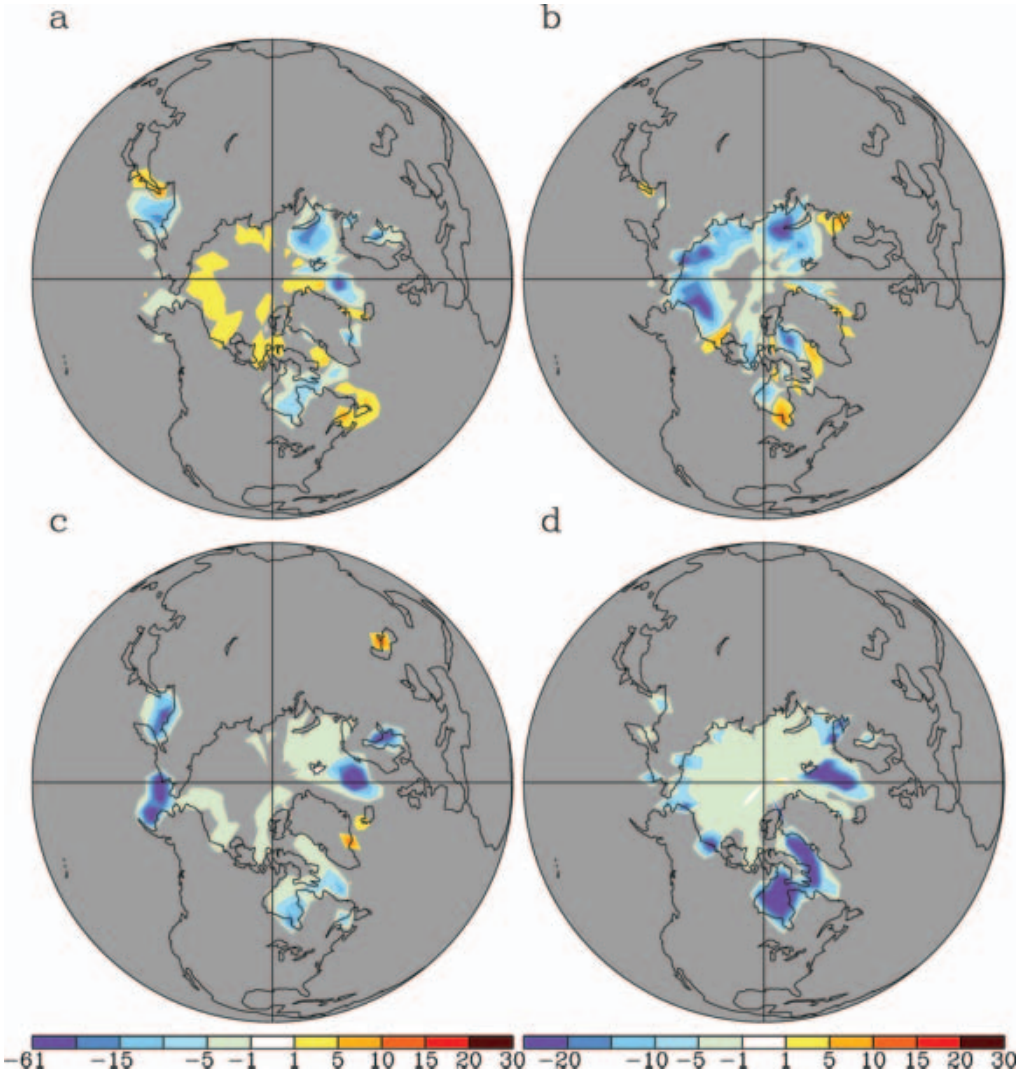

Fig. 1. (a,b) Observed NH sea-ice extent change based on a linear trend (%) for 1978–2004 (Rayner and others, 2003): (a) December–February; (b) June–August. (c,d) Change of NH sea-ice extent (%) in $2 \times CO_2$ experiment ($2 \times CO_2$ experiment minus control): (c) December–February; (d) June–August.

a drift of 0.06°C per century and indicated a global mean SAT of about +14°C at model year 1000. The model climate sensitivity for doubled CO_2 is ~2.7°C, which is within the range 3 ± 1°C for doubled CO_2 inferred from paleoclimate evidence (Hansen and others, 1984, 1993). Two experiments were performed, starting at year 21 of the control, with instantaneous doubling and halving of CO_2 compared to the control run CO_2 level, referred to as the $2 \times CO_2$ and $0.5 \times CO_2$ experiments, respectively.

3. RESULTS

After 120 years of integration, the global mean SAT warmed by 2°C in $2 \times CO_2$ experiments, causing a reduction in sea-ice extent of 15%. Figure 1a and b show the Northern Hemisphere (NH) sea-ice extent change based on a linear trend for 1978–2004 from observational data (Rayner and others, 2003). Analysis of these data, as well as recently reported sea-ice cover change data (Serreze and others, 2003; Johannessen and others, 2004; Rigor and Wallace, 2004; Stroeve and others, 2005), shows a reduction of sea-ice cover in every season, with maximum decrease in summer and autumn. In summer, a decrease in sea-ice extent was observed in both the Eurasian and Canadian basins of the Arctic, while in autumn the largest reduction in sea ice was observed in the Beaufort and Chukchi Seas. The $2 \times CO_2$ experiment reveals a seasonality of sea-ice reduction in the NH consistent with observational data (Fig. 1c and d). The decreases of sea-ice cover are most pronounced (>50%) in the Barents and Greenland Seas, in some areas of the Beaufort and Chukchi Seas and in Baffin Bay. In autumn, the model shows a residual high shrinkage of sea-ice cover as well.

The Arctic SLP data from the Arctic Ocean Buoy Program show a significant decrease in the annual mean SLP every year since 1988 (Walsh and others, 1996). This change in the SLP pattern is reflected in the positive trend of the AO index, which is defined as the leading principal component of the wintertime (November–April) monthly mean SLP field over the domain poleward of 20° N (Thompson and Wallace, 1998). Thompson and Wallace (1998, 2000) and Thompson and others (2000) also suggested that the leading mode of month-to-month variability of the extratropical general circulation in the NH can be characterized as a seesaw of atmospheric mass between polar cap and middle latitudes. There is evidence that the winter AO has had a persistent positive phase since the mid-1970s (Hurrell, 1995;

https://doi.org/10.3189/172756506781828566 Published online by Cambridge University Press

Thompson and Wallace, 1998, 2001). In addition to the positive trend, this period also included an increase in the temporal variability of the AO index (Dickson and others, 2000; Feldstein, 2002; Overland and Wang, 2005). In the positive polarity, the AO is characterized by strong westerlies around the perimeter of the Arctic. The mean meridional circulation shows that during the high AO state the polar cell exhibits an anomalous rising motion over subpolar latitudes, and subsidence between 40°and 50° N (Thompson and Wallace, 2000; Moritz and others, 2002).

Although there is still a question as to whether global warming is responsible for the upward trend in observations of the AO (Osborn and others, 1999), it has been argued that the spatial patterns of the atmospheric circulation response to external forcing may project into modes of natural climate variability such as the AO (Corti and others, 1999; Overland and Wang, 2005). The increased greenhouse gas and decreased stratospheric ozone concentrations are thought to cool the lower stratosphere at high latitudes. Cold lower stratospheric temperatures induce strengthening of the polar vortex and have the potential to increase the AO index (Houghton and others, 2001) since stratospheric wind anomalies are observed to propagate downward. Stratospheric wind anomalies are also highly correlated with zonal wind anomalies at the surface (Perlwitz and Graf, 1995; Baldwin and Dunkerton, 1999). In addition, the theoretical and observational results indicate that the high AO events are accompanied by an anomalous poleward eddy flux of westerly momentum. Under conditions of strengthened polar cell, this acts to maintain the anomalous westerlies at high latitudes, providing a self-supporting mechanism for the AO (Limpasuvan and Hartmann, 1999; Thompson and Wallace, 2000).

The SLP decreases significantly over the polar regions and increases at middle latitudes in the warming scenario, which maintains the seesaw mechanism of atmospheric masses between polar and mid-latitude regions under constant warming conditions. In addition, increasing CO_2 cools the stratosphere and warms the troposphere (fig. 20 of Hansen and others, 2005), which is reflected in a strengthening of the polar cell and enhancement of westerlies poleward of ~40° N (fig. 22 of Hansen and others, 2005) during the NH winter. These two factors create a self-reinforcing mechanism for the positive AO polarity under persistent warming conditions. The $2 \times CO_2$ experiment shows the positive trend of the winter AO (Fig. 2a). The large temporal variability of the AO index demonstrates the ability of our model to reproduce large observed year-to-year changes of Arctic/North Atlantic climate with increased warming.

Figure 3a shows the correlation coefficient between winter (December–March) SAT and AO index. Under warming conditions, the large-scale pattern of SAT variability is similar to that accompanying the AO (Thompson and others, 2000). SAT is positively correlated with the AO over northern Eurasia, southeast USA, the subtropical Atlantic and Pacific and the central Arctic and it is negatively correlated over Greenland, the Labrador Sea, northern Africa, northwestern Canada and the northeastern Pacific. These SAT and AO correlations are consistent with advection by the large-scale atmospheric flow (Thompson and others, 2000). Figure 4a shows that the surface wind anomaly patterns indicate intensification of warm southerly flow over southeast USA, cold northwesterly flow over the Labrador Sea, warm southwesterly flow over northwest Europe and

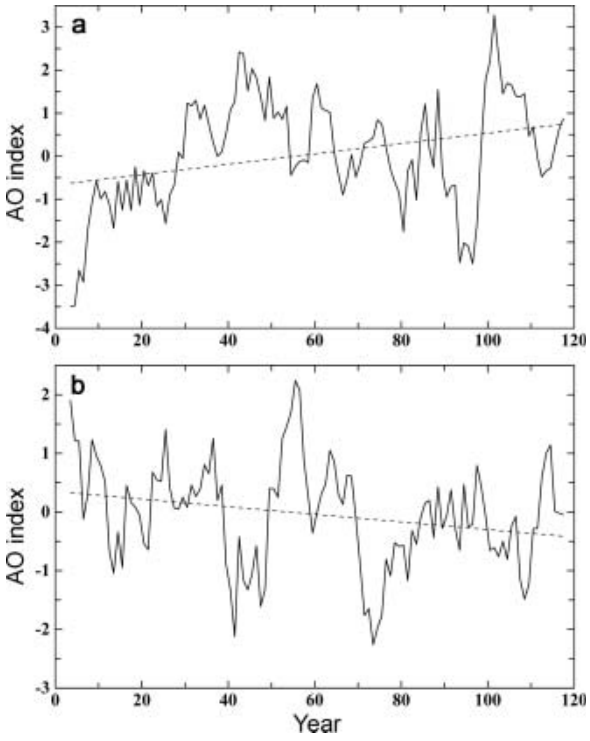

Fig. 2. Winter (November–April) AO index (5 year running mean) and long-term trend: (a) $2 \times CO_2$; (b) $0.5 \times CO_2$.

cold northeasterly flow over the Mediterranean region. The winter sea-ice cover is inversely correlated with the winter AO (Fig. 3c), with two areas of positive correlation with the AO index. These areas, off the east coast of Greenland and in the Labrador Sea, are associated with the enhanced advection of sea ice under the AO trend toward high-index polarity, which was also noted from the analysis of the International Arctic Buoy Programme data (Rigor and others, 2006). The largest anticorrelations between the AO index and sea-ice extent are along the Siberian sector of the Arctic, which resulted from a great decrease of sea ice through a combination of advection and melt. Due to significantly reduced sea-level pressure over the central Arctic, the cyclone activity north of Siberia has increased during the high-index conditions of the AO, which favors stronger and more frequent warm southerly winds (Fig. 4a). These southerly winds from the area of maximum positive correlation between the AO index and SAT over northern Eurasia (Figs 3a and 4a) contribute to increased sea-ice melting and to advection of ice poleward from the coast. In addition, the increased cyclone activity over the central Arctic is believed to promote ice divergence (Maslanik and others, 1996; Serreze and others, 2003; Rigor and others, 2006).

We ran an ensemble of five model simulations beginning in AD 1880 and extending through 2002, driven by increasing well-mixed greenhouse gases, solar irradiance, stratospheric water vapor derived from methane oxidation, tropospheric and stratospheric ozone, volcanic aerosols, changes in land use and snow/ice albedo change proportional to the local soot deposition (Hansen and others, 2005). A decrease, from about 4.49% of the Earth's surface to about 4.2%, of ocean ice cover area over the past century is simulated. The observational data (Rayner and others, 2003) show a decrease of sea-ice cover from about 4.55% to about 4.1%. The model reproduces the global sea-ice cover

https://doi.org/10.3189/172756506781828566 Published online by Cambridge University Press

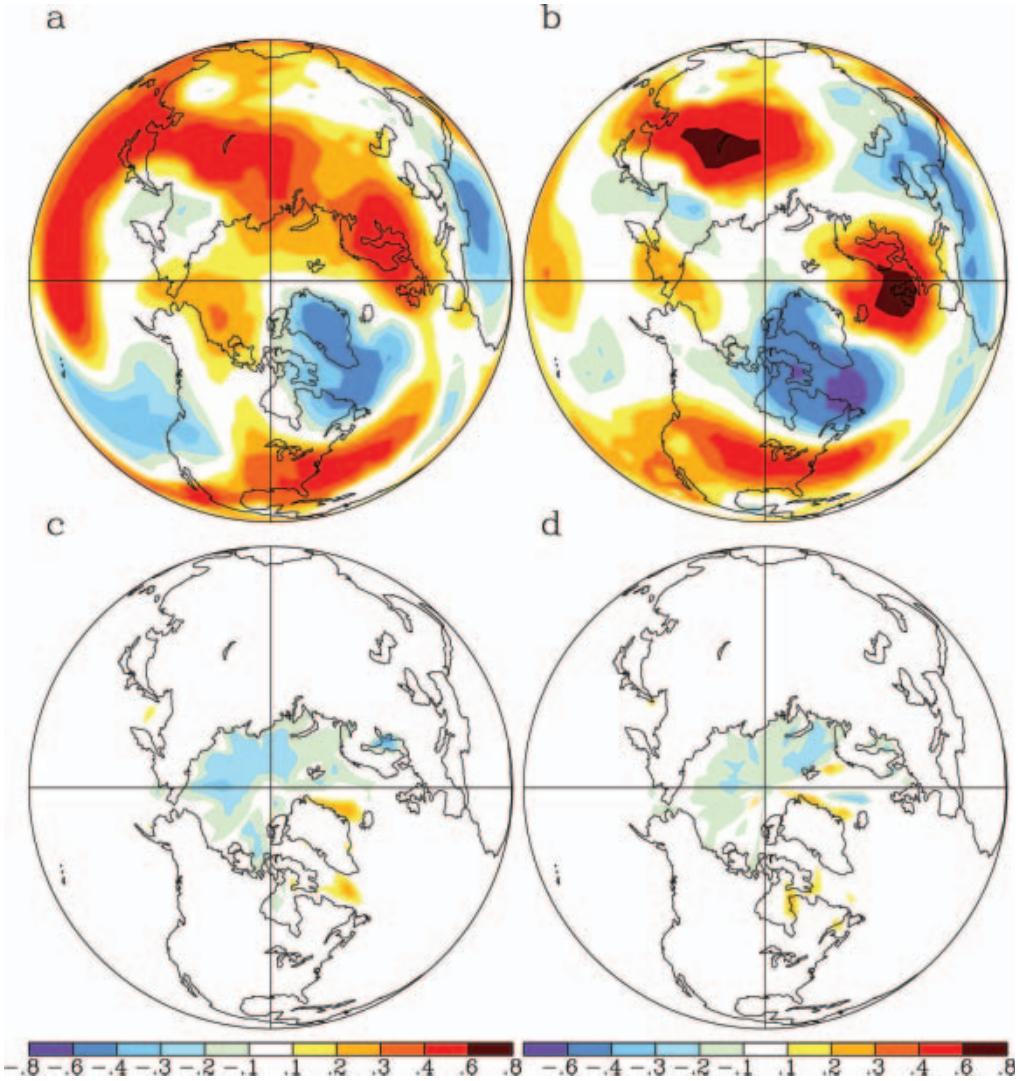

Fig. 3. (a,b) Correlation coefficient between December–March NH SAT and AO index: (a) $2 \times CO_2$; (b) $0.5 \times CO_2$. (c,d) Correlation coefficient between December–March NH sea-ice concentration and AO index: (c) $2 \times CO_2$; (d) $0.5 \times CO_2$. Note the decimal point in the scale.

well and sea ice is more stable in the present model than in previous GISS models.

Due to extensive sea-ice melting, enhanced ice advection from the central Arctic and increased precipitation, the salinity of the surface ocean layer indicated by our simulation decreased by about 1 psu (practical salinity unit) in the central Arctic, the Labrador Sea and the North Atlantic. All these factors contributed to the fact that under warming conditions MOC in the North Atlantic weakens and becomes much shallower (Fig. 5a) such that from a depth of about 2000 m to the bottom the water is ventilated from the Southern Ocean as the reverse overturning cell of Antarctic Bottom Water (AABW) intensifies and penetrates northward up to 40–45° N. As was noted in earlier studies (Manabe and Stouffer, 1999; Wood and others, 1999), the MOC weakening is attributable mainly to ocean freshening in high latitudes as a result of strong sea-ice melting and ocean warming. The sea surface temperature (SST) increased by several degrees over most of the North Atlantic, with the maximum SST warming in the Norwegian Sea. The $2 \times CO_2$ experiment exhibits the region of SST cooling, which is located to the southeast of Greenland. Both weakening of North Atlantic MOC and reduction of the northward ocean heat transport by the Gulf Stream are important in modifying the ocean surface response to warming conditions. This was noted in other studies (Russell and Rind, 1999; Wood and others, 1999; Hu and others, 2004) and may explain the SST cooling in this region.

As a consequence of the weakened MOC indicated by the model, the northward heat transport is reduced due to weakened flow in the Gulf Stream. The weak Gulf Stream extends only to about 40° N, whereas the cyclonic circulation of the surface ocean layer in the Greenland, Iceland and Norwegian seas intensifies. The stronger East Greenland Current of this cyclonic gyre supplies freshened Arctic Ocean water to the North Atlantic region along the West Greenland coast. The intensification of upper-ocean cyclonic circulation in the Greenland, Iceland and Norwegian seas is caused by an increase in surface wind along the European coast as well as by amplification of westerlies in the North Atlantic (Fig. 4a). The enhanced westerly flow across the North Atlantic brings warm, moist air over the northern part of Russia and Scandinavia, which results in increased precipitation. At the same time, drier conditions under warming scenarios are obtained over central and southern Europe, the Mediterranean and the Middle East. From the experiments with increased CO_2 concentration, the results show weakening in the Atlantic thermohaline

https://doi.org/10.3189/172756506781828566 Published online by Cambridge University Press

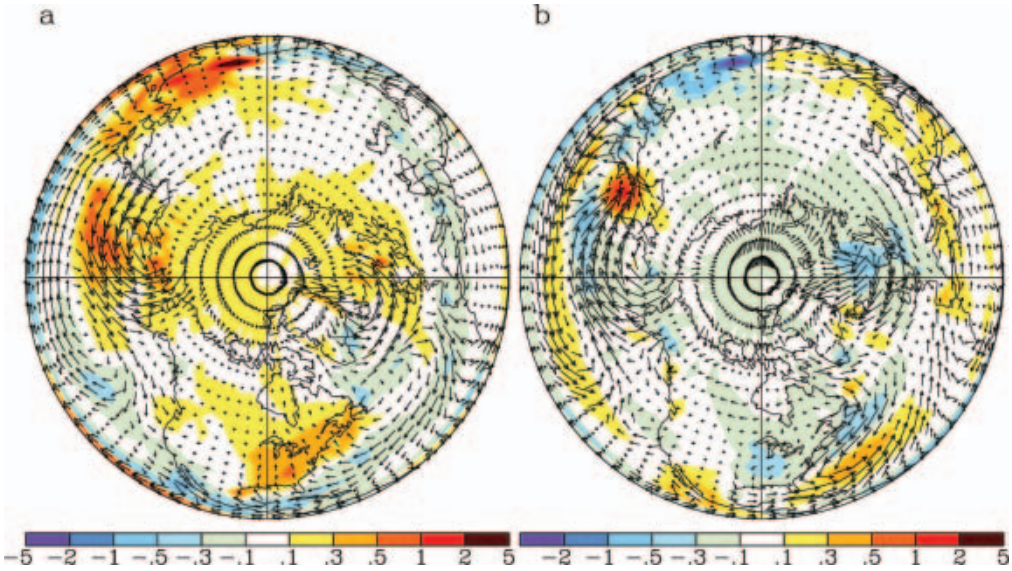

Fig. 4. Change of precipitation (mm d^{-1}). Vectors are for the change in surface wind (m s^{-1}). (a) 2 × CO_2; (b) 0.5 × CO_2. All the changes are significant at the 95% level. Note the decimal point in the scale.

circulation and atmospheric conditions favoring a positive phase in the NAO. This in turn contributes even more to increased precipitation minus evaporation and freshening at high northern latitudes.

For the CO_2-reduced (0.5 × CO_2) experiments, the global mean (40 year) SAT is 1.8°C lower than in the control experiments. The largest cooling is found in the high latitudes of the NH (fig. 18 of Hansen and others, 2005). A large cooling of the troposphere and warming of the stratosphere in the high northern latitudes (fig. 20 of Hansen and others, 2005) leads to increased SLP in these regions. The increased SLP over polar latitudes causes substantial weakening of the polar cell, which is immediately reflected by weakened westerlies poleward of ~40° N (fig. 22 of Hansen and others, 2005) during the winter. These self-sustaining conditions of cooling and increase in SLP over the Arctic are reproduced in the negative overall trend of the winter AO index (Fig. 2b), although the model again reproduces large year-to-year variability under extreme cooling. Comparison of sea-ice extent and AO index shows that the anticorrelations are stronger in the European sector of the Arctic (Fig. 3d). This finding is confirmed by the analysis of the sea-ice extent and negative phase of the NAO and AO oscillations (Dickson and others, 2000; Thompson and others, 2000; Rigor and others, 2006), and explained by strengthening anticyclonic activity over the central Arctic and reduction of sea-ice export from the European Arctic. The cooling conditions lead to thicker and more extensive sea ice. In the Southern Hemisphere, the increase in sea-ice area (28%) dominates over the ice-thickness increase (5%) due to open ocean in the equatorward direction, which is favorable for sea-ice spread and which prevents sea ice from thickening. In the NH, sea-ice area increased by only 8% due to the enclosed land/sea configuration, but it became much thicker (108%).

The SAT and AO correlations (Fig. 3b) result from increased SLP over the polar regions. Increased SLP causes weaker westerly flow across the North Atlantic and reduced penetration of maritime air over northern Europe (Fig. 4b). In the tropical and subtropical Atlantic, the northward shift of the Inter-Tropical Convergence Zone causes strengthening of the southwesterly wind flow across the subtropical Atlantic. This brings moist maritime air masses over southern Europe and northern Africa and leads to increased precipitation over these regions. Precipitation and evaporation decrease almost everywhere due to the colder climate. However, stronger surface winds over the Labrador Sea and subtropical Atlantic favor increased evaporation over these areas, which makes the surface water more saline and contributes to the strengthening of deep convection in the North Atlantic.

Under cooling conditions, the MOC becomes stronger (Fig. 5b). The southward shift of the convection sites is consistent with other modeling studies and paleoceanographic data (Sarnthein and others, 1994; Ganopolski and others, 1998; Hewitt and others, 2001; Shin and others, 2003; Liu and others, 2005). Increased northward heat transport is a consequence of stronger Atlantic MOC, which is seen in an intensification of the Gulf Stream and stronger circulation in the subtropical Atlantic. Enhanced overturning circulation in the northern and subtropical Atlantic and a stronger Gulf Stream contribute to more northward heat transport and maintain relatively warm SSTs in the northern part of the North Atlantic. In the Southern Ocean, cooling experiments show an increase in overturning circulation as well, which may lead to a situation in which deep ocean layers of AABW become sufficiently dense that, after penetration into the deep North Atlantic, vertical stability

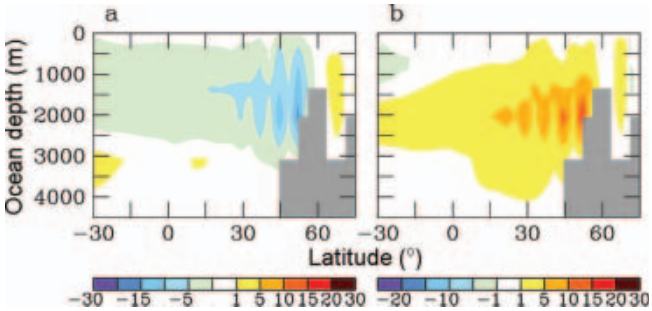

Fig. 5. Change of the meridional mass transport stream function in the Atlantic Ocean (Sv): (a) 2 × CO_2 (b) 0.5 × CO_2. All changes are significant at the 95% level.

https://doi.org/10.3189/172756506781828566 Published online by Cambridge University Press

is increased, thus preventing surface water from sinking as deeply in the North Atlantic. Recent paleoclimate data indicate evidence of a Southern Ocean lead over the NH climate by 1000–2000 years for glacial cycles (Wunsch, 2003). However, for the shorter timescales the hemispheres are not coupled, and the decade-to-century Atlantic variability is controlled by the North Atlantic itself through its fast adjustment (Stocker, 2000; Stouffer, 2004).

4. CONCLUSIONS

The primary causal mechanism that drives the AO towards its high index polarity still remains to be determined. Some authors (Hurrell, 1996; Thompson and others, 2000) hypothesize that anthropogenic forcing may be a contributing factor to the recent strengthening of the polar vortex (reflected by the AO) and warming over the NH continents. The SLP decrease over polar latitudes and increase south of about 50° N (reflected in strengthening of the polar cell and enhancement of westerlies around the perimeter of the Arctic, as well as in cooling of the stratosphere and warming of the troposphere) create a self-supporting mechanism for the positive AO phase under the warming scenario. A trend towards a positive phase of the AO oscillation in the $2 \times CO_2$ experiment is in agreement with previously published reports on the AO trend towards higher values with increasing greenhouse gas concentration (Fyfe and others, 1999; Gillett and others, 2002; Osborn, 2004). The typical warming pattern in the atmosphere is reflected in an anomalously strong NH atmospheric circulation with a pattern of Atlantic variability that is very similar to the observations (Hurrell, 1995; Wallace and others, 1995; Timmermann and others, 1998). In addition this NAO-like pattern (SLP decrease over the Arctic and SLP increase at middle latitudes) includes an intensification of westerlies in the North Atlantic, which results in increased precipitation over northern Europe and decreased precipitation over central and southern Europe, the Mediterranean and the Middle East. Large temporal variability of the AO index confirms recently reported observational evidence of this phenomenon under increased warming during the past few decades (Dickson and others, 2000; Feldstein, 2002; Overland and Wang, 2005). SAT increase caused reduction of sea-ice cover by 15%, with the largest decrease in summer and autumn, consistent with recently reported analyses of the Arctic sea-ice cover change (Rayner and others, 2003; Serreze and others, 2003; Johannessen and others, 2004; Rigor and Wallace, 2004; Stroeve and others, 2005). The increased fresh-water flux from sea-ice melting and from enhanced precipitation over high latitudes contributes to upper ocean stratification in areas of deep water formation, which is reflected in the weakening of the North Atlantic MOC.

The CO_2-reduced experiment exhibits an SLP increase over the high latitudes and SLP decrease over middle latitudes, which cause substantial weakening of the polar cell and westerlies poleward of ~40° N. The corresponding shift of the AO index towards its low index phase is a result of a self-supporting mechanism due to tropospheric cooling and stratospheric warming as well as SLP increase over the Arctic. During negative AO conditions, lower temperatures and weaker westerly flow across the North Atlantic cause reduction of precipitation over northern Europe and Russia. Strengthening the southwesterly wind flow across the subtropical Atlantic contributes to the increase in precipitation over southern Europe, the Mediterranean and northern Africa. Overall cooling and strengthening of the anticyclonic circulation over the central Arctic contributes to the extension and thickening of the sea-ice cover. Under CO_2-induced cooling conditions, the North Atlantic itself controls the Atlantic thermohaline circulation and climate due to its fast adjustment on decadal-to-century timescales, which is reflected in an intensified and deepened North Atlantic overturning cell.

ACKNOWLEDGEMENTS

We acknowledge support from the NASA Earth Science Research Division. We thank J. Lerner for technical assistance with the plots.

REFERENCES

Baldwin, M.P. and T.J. Dunkerton. 1999. Propagation of the Arctic Oscillation from the stratosphere to the troposphere. *J. Geophys. Res.,* **104**(D24), 30,937–30,946.

Belchansky, G.I., D.C. Douglas, V.A. Eremeev and N.G. Platonov. 2005. Variations in the Arctic's multiyear sea ice cover: a neural network analysis of SMMR-SSM/I data, 1979–2004. *Geophys. Res. Lett.,* **32**(9), L09605. (10.1029/2005GL022395.)

Comiso, J.C. 2002. A rapidly declining perennial sea ice cover in the Arctic. *Geophys. Res. Lett.,* **29**(20), 1956. (10.1029/2002GL015650.)

Corti, S., F. Molteni and T.N. Palmer. 1999. Signature of recent climate change in frequencies of natural atmospheric circulation regimes. *Nature,* **398**(6730), 799–802.

Curry, J.A., W.B. Rossow, D. Randall and J.L. Schramm. 1996. Overview of Arctic cloud and radiation characteristics. *J. Climate,* **9**(19), 1731–1765.

Deser, C., J.E. Walsh and M.S. Timlin. 2000. Arctic sea ice variability in the context of recent atmospheric circulation trends. *J. Climate,* **13**(3), 617–633.

Dickson, R.R. *and 8 others*. 2000. The Arctic Ocean response to the North Atlantic Oscillation. *J. Climate,* **13**(15), 2671–2696.

Fang, Z.F. and J.M. Wallace. 1994. Arctic sea ice variability on a timescale of weeks and its relation to atmospheric forcing. *J. Climate,* **7**(12), 1897–1914.

Feldstein, S.B. 2002. The recent trend and variance increase of the annular mode. *J. Climate,* **15**(11), 88–94.

Fyfe, J.C., G.J. Boer and G.M. Flato. 1999. The Arctic and Antarctic oscillations and their projected changes under global warming. *Geophys. Res. Lett.,* **26**(11), 1601–1604.

Ganopolski, A., S. Rahmstorf, V. Petoukhov and M. Claussen. 1998. Simulation of modern and glacial climates with a coupled global model of intermediate complexity. *Nature,* **391**(6665), 351–356.

Gent, P.R. and J.C. McWilliams. 1990. Isopycnal mixing in ocean circulation models. *J. Phys. Oceanogr.,* **20**(1), 150–155.

Gillett, N.P., M.R. Allen, R.E. McDonald, C.A. Senior, D.T. Shindell and G.A. Schmidt. 2002. How linear is the Arctic Oscillation response to greenhouse gases? *J. Geophys. Res.,* **107**(D3), 4022. (10.1029/2001JD000589.)

Hansen, J. *and 7 others*. 1984. Climate sensitivity: analysis of feedback mechanisms. *In* Hansen, J.E. and T. Takahashi, *eds. Climate processes and climate sensitivity.* Washington, DC, American Geophysical Union, 130–163. (Geophysical Monograph 29.)

Hansen, J., A. Lacis, R. Ruedy, M. Sato and H. Wilson. 1993. How sensitive is the world's climate? *Natl. Geogr. Res. Explor.,* **9**, 142–158.

Hansen, J. *and 27 others*. 2002. Climate forcings in Goddard Institute for Space Studies SI2000 simulations. *J. Geophys. Res.,* **107**(D18), 4347. (10.1029/2001JD001143.)

Hansen, J. *and 45 others*. 2005. Efficacy of climate forcings. *J. Geophys. Res.,* **110**(D18), D18104. (10.1029/2005JD005776.)

https://doi.org/10.3189/172756506781828566 Published online by Cambridge University Press

Hewitt, C.D., A.J. Broccoli, J.F.B. Mitchell and R.J. Stouffer. 2001. A coupled model study of the last glacial maximum: Was part of the North Atlantic relatively warm? *Geophys. Res. Lett.,* **28**(8), 1571–1574.

Holland, M.M. and C.M. Bitz. 2003. Polar amplification of climate change in coupled models. *Climate Dyn.,* **21**(3–4), 221–232.

Houghton, J.T. *and 7 others*. 2001. *Climate change 2001: the scientific basis. Contribution of Working Group I to the Third Assessment Report of the Intergovernmental Panel on Climate Change.* Cambridge, etc. Cambridge University Press.

Hu, A., G.A. Meehl, W.M. Washington and A. Dai. 2004. Response of the Atlantic thermohaline circulation to increased atmospheric CO_2 in a coupled model. *J. Climate,* **17**(21), 4267–4279.

Hurrell, J.W. 1995. Decadal trends in the North Atlantic Oscillation: regional temperature and precipitation. *Science,* **269**(5224), 676–679.

Hurrell, J.W. 1996. Influence of variations in extratropical wintertime teleconnections on Northern Hemisphere temperature. *Geophys. Res. Lett.,* **23**(6), 665–668.

Johannessen, O.M. *and 11 others*. 2004. Arctic climate change: observed and modeled temperature and sea-ice variability. *Tellus,* **56A**(4), 328–341.

Large, W.G., J.C. Williams and S.C. Doney. 1994. Oceanic vertical mixing: a review and a model with a nonlocal boundary layer parameterization. *Rev. Geophys.,* **32**(4), 397–422.

Limpasuvan, V. and D.L. Hartmann. 1999. Eddies and the annular modes of climate variability. *Geophys. Res. Lett.,* **26**(20), 3133–3136.

Liu, Z., S.I. Shin, R.S. Webb, W. Lewis and B.L. Otto-Bliesner. 2005. Atmospheric CO_2 forcing on glacial thermohaline circulation and climate. *Geophys. Res. Lett.,* **32**(2) L02706. (10.1029/2004GL021929.)

Manabe, S. and R.J. Stouffer. 1999. The role of thermohaline circulation in climate. *Tellus,* **51A–B**(1), 91–109.

Manabe, S., M.J. Spelman and R.J. Stouffer. 1992. Transient responses of a coupled ocean–atmosphere model to gradual changes of atmospheric CO_2. Part II: Seasonal response. *J. Climate,* **5**(2), 105–126.

Maslanik, J.A., M.C. Serreze and R.G. Barry. 1996. Recent decreases in Arctic summer ice cover and linkages to atmospheric circulation anomalies. *Geophys. Res. Lett.,* **23**(13), 1677–1680.

Moritz, R.E., C.M. Bitz and E.J. Steig. 2002. Dynamics of recent climate change in the Arctic. *Science,* **297**(5586), 1497–1502.

Osborn, T.J. 2004. Simulating the winter North Atlantic Oscillation: the roles of internal variability and greenhouse gas forcing. *Climate Dyn.,* **22**, 605–623.

Osborn, T.J., K.R. Briffa, S.F.B. Tett, P.D. Jones and R.M. Trigo. 1999. Evaluation of the North Atlantic Oscillation as simulated by a coupled climate model. *Climate Dyn.,* **15**(9), 685–702.

Overland, J.E. and M. Wang. 2005. The Arctic climate paradox: the recent decrease of the Arctic Oscillation. *Geophys. Res. Lett.,* **32**(6), L06701. (10.1029/2004GL021752.)

Parkinson, C.L. and D.J. Cavalieri. 2002. A 21 year record of Arctic sea-ice extents and their regional, seasonal and monthly variability and trends. *Ann. Glaciol.,* **34**, 441–446.

Perlwitz, J. and H.F. Graf. 1995. The statistical connection between tropospheric and stratospheric circulation of the Northern Hemisphere in winter. *J. Climate,* **8**(10), 2281–2295.

Randall, D. *and 9 others*. 1998. Status of and outlook for large-scale modeling of atmosphere–ice–ocean interactions in the Arctic. *Bull. Am. Meteorol. Soc.,* **79**(2), 197–219.

Rayner, N.A. *and 7 others*. 2003. Global analyses of sea surface temperature, sea ice, and night marine air temperature since the late nineteenth century. *J. Geophys. Res.,* **108**(D14), 4407. (10.1029/2002JD002670.)

Rigor, I.G. and J.M. Wallace. 2004. Variations in the age of Arctic sea-ice and summer sea-ice extent. *Geophys. Res. Lett.,* **31**(9), L09401. (10.1029/2004GL019492.)

Rigor, I.G., J.M. Wallace and R.L. Colony. 2006. Response of sea ice to the Arctic Oscillation. *J. Climate,* **15**(18), 2648–2663.

Rind, D. 1998. Latitudinal temperature gradients and climate change. *J. Geophys. Res.,* **103**(D6), 5943–5972.

Russell, G.L. and D. Rind. 1999. Response to CO_2 transient increase in the GISS coupled model: regional coolings in a warming climate. *J. Climate,* **12**(2), 531–539.

Sarnthein, M. *and 6 others*. 1994. Changes in east Atlantic deepwater circulation over the last 30,000 years: eight time slice reconstructions. *Paleoceanography,* **9**(2), 209–267.

Schmidt, G.A. *and 35 others*. 2006. Present-day atmospheric simulations using GISS ModelE: comparison to in-situ, satellite, and reanalysis data. *J. Climate,* **19**(2), 153–192.

Serreze, M.C. *and 9 others*. 2003. A record minimum sea ice cover in the Arctic Ocean for summer 2002. *Geophys. Res. Lett.,* **30**(3), 1110. (1029/2002GL016406.)

Shin, S.I., Z. Liu, B.L. Otto-Bliesner, J.E. Kutzbach and S.J. Vavrus. 2003. Southern Ocean sea-ice control of the glacial North Atlantic thermohaline circulation. *Geophys. Res. Lett.,* **30**(2). (10.1029/2002GL015513.)

Slonosky, V.C., L.A. Mysak and J. Derome. 1997. Linking arctic sea ice and atmospheric circulation anomalies on interannual and decadal time scales. *Atmos.–Ocean,* **35**, 333–366.

Stocker, T.F. 2000. Past and future reorganizations in the climate system. *Quat. Sci. Rev.,* **19**, 301–319.

Stouffer, R.J. 2004. Time scales of climate response. *J. Climate,* **17**(1), 209–217.

Stroeve, J.C. *and 6 others*. 2005. Tracking the Arctic's shrinking ice cover: another extreme September minimum in 2004. *Geophys. Res. Lett.,* **32**(4) L04501). (10.1029/2004GL021810.)

Thompson, D.W.J. and J.W. Wallace. 1998. The Arctic Oscillation signature in the wintertime geopotential height and temperature fields. *Geophys. Res. Lett.,* **25**(9), 1297–1300.

Thompson, D.W.J. and J.M. Wallace. 2000. Annular modes in the extratropical circulation. Part I: Month-to-month variability. *J. Climate,* **13**(5), 1000–1016.

Thompson, D.W.J. and J.M. Wallace. 2001. Regional climate impacts of the Northern Hemisphere annuluar mode. *Science,* **293**(5527), 85–89.

Thompson, D.W.J., J.M. Wallace and G.C. Hegerl. 2000. Annular modes in the extratropical circulation. Part II: Trends. *J. Climate,* **13**(5), 1018–1036.

Timmermann, A., M. Latif, R. Voss and A. Grötzner. 1998. Northern hemispheric interdecadal variability: a coupled air–sea mode. *J. Climate,* **11**(8), 1906–1931.

Wallace, J.M., Y. Zhang and J.A. Renwick. 1995. Dynamic contribution to hemispheric mean temperature trends. *Science,* **270**(5237), 780–783.

Walsh, J.E., W.L. Chapman and T.L. Shy. 1996. Recent decrease of sea level pressure in the central Arctic. *J. Climate,* **9**(2), 480–486.

Walsh, J.E., V.M. Kattsov, W.L. Chapman, V. Govorkova and T. Pavlova. 2002. Comparison of Arctic climate simulations by uncoupled and coupled global models. *J. Climate,* **15**(12), 1429–1446.

Wood, R.A., A.B. Keen, J.F.B. Mitchell and J.M. Gregory. 1999. Changing spatial structure of the thermohaline circulation in response to atmospheric CO_2 forcing in a climate model. *Nature,* **399**(6736), 572–575.

Wunsch, C. 2003. Greenland–Antarctic phase relations and millennial time-scale climate fluctuations in the Greenland ice-cores. *Quat. Sci. Rev.,* **22**(15), 1631–1646.

MS received 3 November 2005 and accepted in revised form 22 June 2006